UNIVERSITY OF CALIFORNIA

Ernest O. Lawrence

Radiation Laboratory

LIVERMORE SITE

DISCLAIMER

UCRL-5946

UNIVERSITY OF CALIFORNIA

Lawrence Radiation Laboratory

Livermore, California

Contract No. W-7405-eng-48

ANGULAR DISTRIBUTION OF THE GROUND-STATE NEUTRONS FROM THE $C^{13}(p,n)N^{13}$ AND $N^{15}(p,n)O^{15}$ REACTIONS

C. Wong, J.D. Anderson, S.D. Bloom, J.W. McClure,

and B.D. Walker

January 23, 1961

BLANK PAGE

Angular Distribution of the Ground-State Neutrons from the $C^{13}(p,n)N^{13}$ and $N^{15}(p,n)O^{15}$ Reactions*†

C. WONG, J.D. ANDERSON, S.D. BLOOM, J.W. McCLURE,

AND B.D. WALKER

Lawrence Radiation Laboratory, University of California

Livermore, California

January 23, 1961

ABSTRACT

The angular distribution of the neutrons from the $C^{13}(p,n)N^{13}$ and $N^{15}(p,n)O^{15}$ ground-state reactions has been measured in 10° steps from 0° to 150° for incident proton (laboratory) energies of approximately 6.5, 6.9, 7.5, 8.1, 8.6, 8.9, 9.4, 10.6, 11.4, and 12.2 Mev. Additional measurements were made for C^{13} at 5.0, 10.2, 10.9, and 13.3 Mev, and for N^{15} at 5.5, 7.7, 7.8, and 13.6 Mev. A calibrated plastic or stilbene scintillator was used in order to obtain absolute differential cross sections. Time-of-flight techniques on the Livermore variable-energy cyclotron allowed positive identification of the ground-state neutrons. The targets $\left[CO_2(58\%\ C^{13})\right.$ and $\left.N_2(90\%\ N^{15})\right]$ were sufficiently thick to average out the effects of possible compound-nucleus contributions. From preliminary fits to the C^{13} angular distributions, Glendenning and Bloom have inferred an effective neutron-proton interaction inside the nucleus.

BLANK PAGE

Angular Distribution of the Ground-State Neutrons from the $C^{13}(p,n)N^{13}$ and $N^{15}(p,n)O^{15}$ Reactions

C. WONG, J. D. ANDERSON, S. D. BLOOM, J. W. McCLURE, AND B. D. WALKER

Lawrence Radiation Laboratory, University of California
Livermore, California

INTRODUCTION

It has been suggested by Bloom, Glendenning, and Moszkowski[1] that one may be able to deduce the effective neutron-proton interaction inside a nucleus by studying the ground-state (p,n) reactions on mirror nuclei. The $N^{15}(p,n)O^{15}$ ground-state reaction has been investigated by Jones et al.[2] from threshold up to 6.4-Mev proton energy. They measured the relative angular distribution of the ground-state neutrons at selected energies, as well as the absolute zero-degree excitation function. The $C^{13}(p,n)N^{13}$ ground-state absolute neutron yield has been measured by Gibbons and Macklin[3] from threshold up to a proton energy of 5.3 Mev. Utilizing activation techniques, Blaser et al.[4] and Bloom et al.[5] have measured the $C^{13}(p,n)N^{13}$ ground-state yield from threshold up to 6.7 Mev and up to 11.3 Mev, respectively. Zero-degree neutron yields from C^{13}+p have been measured up to 5 Mev by Bair et al.,[6] and up to 8.7 by Dagley et al.[7] The relative angular distribution of the $C^{13}(p,n)N^{13}$ ground-state neutrons has been measured by Albert et al.[8] from threshold up to 5.3 Mev utilizing a BF_3 "long" counter, and by Bair et al.[9] from 3.5- to 4.6-Mev proton energy utilizing a propane recoil counter. Above 5.3 Mev, the long-counter results might be ambiguous since neutrons from the breakup of C^{13} would be

detected if present; above 5.78-Mev proton energy, the long counter would detect, if present, the neutrons leaving N^{13} in its first excited state.[10]

With the use of time-of-flight techniques,[11] the C^{13} and N^{15}(p, n) ground-state neutron angular distributions have been measured up to a proton energy of 13.6 Mev. Time-of-flight techniques readily separate the ground-state neutrons from break-up neutrons (p;p'n) and from neutron groups leaving N^{13} and O^{15} in excited states. Higher proton bombarding energies are preferable since it is expected that direct reactions will predominate.

EXPERIMENTAL METHOD

Geometry

The experimental geometry is shown in Fig. 1. From 5.0- to 8.6-Mev proton energy, a 3/4-in.-diameter by 2-in.-long gas cell was used, while from 8.8 to 13.6 Mev a 1-1/2-in. by 4-in. gas cell was used. The collimator separations, materials, and sizes are as indicated in Fig. 1. Collimators A and B were shielded with lead in order to reduce the intensity of the gamma radiation at the detector. At the higher bombarding energies, the 4.4-Mev carbon gamma ray was copiously produced from these collimators. Typical flight paths varied between 1.5 meters at 6.5-Mev bombarding energy to 2.5 meters at 13.3 Mev. The flight path was increased at the higher bombarding energies in order to prevent the ground-state neutron peak from coinciding in time with the gamma peak from collimator A (see Fig. 3). The detector was mounted on a remotely controlled angle changer. The efficiency of the plastic and stilbene scintillators as a function of neutron energy was calculated and also measured employing the known cross sections for the production of (p + t) and (d + d) neutrons.

Targets

The gas cells were designed to minimize neutron absorption (less than 5%) throughout the angular range between 0 and 150 degrees. The C^{13} was obtained in the form of $BaCO_3$ (58% C^{13}), converted to CO_2, and dried. The N^{15} was obtained in gaseous form (90% N^{15}). Samples of the gases were analyzed for isotopic abundance by mass spectrometry before and after a series of angular-distribution measurements. The gas targets were filled to slightly under atmospheric pressure and were sufficiently thick to "average out"[12] the interference effects between possible compound nucleus and direct interaction contributions. This averaging procedure is meaningful and effective only if the direct-interaction angular distribution is itself a slowly varying function of proton energy . . . i. e., slowly varying compared with the energy spreads introduced by the gas targets.

Electronics

A schematic diagram of the electronics is shown in Fig. 2. The solid portion of the diagram is conventional and has been described in a previous paper.[11] It was discovered that at a proton bombarding energy above 10 Mev there was appreciable gamma-ray background from the shielded collimators and from neutron-capture gamma rays. To suppress the gamma radiation a proton-electron discrimination circuit[13] was introduced as shown in the dashed portion of the diagram. The circuit distinguishes between electron- and proton-induced pulses; a gate is produced if the pulse was induced by a recoil proton. By gating the 256-channel pulse-height analyzer with the coincidence output between slow channel and recoil proton gate, one can effectively suppress the gamma-ray background.

RESULTS

The time-of-flight spectrum for $C^{13} + p$ at 0° and 11.4-Mev protons is shown in Fig. 3. The 5/8-in.-collimator (B in Fig. 1) gamma ray appears twice, since a double display is employed — one converter stop pulse for every two rf cycles. Clearly visible also are the gamma rays from the target and collimator C (unresolved), 3/4-in.-collimator (A in Fig. 1) gamma ray, and neutron groups leaving N^{13} in its ground and various excited states.[10] The crosses and circles represent data taken without and with gamma suppression, respectively. It is seen that the time-independent background (which is due mainly to neutron-capture gamma rays) is suppressed by a factor of twenty-five, while the target gamma ray is suppressed by a factor of one-hundred. The suppression is less for the capture gamma rays because they are higher in energy than the collimator gamma rays and hence have a greater probability of pile-up to produce a false proton-recoil gate.

Figure 4 shows the time-of-flight spectrum for $N^{15} + p$ at 0° and 11.4-Mev protons, employing the gamma suppression circuit. Neutrons from the first excited state[10] are not visible, since if present their energy is below our detector bias of 3.15 Mev. The counts in the region of channel 20-40 are not due to break-up neutrons from the N^{15}, because the bombarding energy is below the threshold for N^{15} breakup. From timing considerations, the counts are consistent with (p,n) reactions from the C^{13} in carbon collimator B.

The center-of-mass absolute differential cross sections for $N^{15}(p,n)$ and $C^{13}(p,n)$ ground-state neutrons are displayed in Figs. 5 and 6. The C^{13} angular distribution at 5.0 Mev is in reasonable agreement with the long-counter results of Albert et al.[8] displayed in Fig. 10. The errors shown reflect "relative" errors, and are an indication of the accuracy obtained in determining the shape of the angular distribution. Relative errors are compounded

from counting statistics and from the reproducibility of the zero-degree cross section measured before and after an angular-distribution measurement. In general, relative errors were of the order of 5% or less, while absolute errors on the differential cross sections were of the order of 10% or less. The proton energy spreads due to energy loss in the gas targets for the various measurements are given in Figs. 5 and 6. In several instances, the angular distributions do vary appreciably when the proton energy is changed by an amount comparable to the energy spread. (A good example is the "flip" in the C^{13} angular distribution between 6.4- and 6.8-Mev proton energy.) These particular angular distributions must be treated with reservation since they represent angular distributions averaged over the energy region of interest. Additional measurements with thinner targets are desirable in these regions.

The angular distributions were integrated to give the total ground-state yield of neutrons. The results are displayed in Fig. 7. The results of Blaser et al.[4] for C^{13} are shown plotted as a solid line from threshold up to 6.7 Mev. In the region of overlap, there is good agreement between the two experiments. The dashed lines were drawn in to illustrate the gross structure of the total excitation functions; obviously, more measurements with thinner targets are needed to bring out any detailed structure in these curves.

As a check on the absolute differential cross sections of Figs. 5 and 6, independent excitation functions for C^{13} and N^{15} at 5° and 40° were determined utilizing the 2-in. gas targets. The results, displayed in Figs. 8 and 9, are in agreement with the results obtained from the earlier absolute angular-distribution measurements. The C^{13} five-degree differential cross section at 5.0 Mev is in excellent agreement with the measurements of Dagley et al.[7] The N^{15} five-degree differential cross sections at 4.85 and 5.5 Mev are in

reasonable agreement with the results of Jones et al.[2] The dashed lines are smooth curves through the measured points, and are intended to show the general trends of the differential excitation functions. It is evident that the positions of the peaks are not too well defined, and detailed structure could be missed because of the wide energy gap between some of the measurements.

DISCUSSION

Since the present work yields not only angular distributions but absolute excitation cross sections as a function of energy as well, one can draw at least qualitative conclusions from both these aspects of the data. The object is to see if both do indeed tend to corroborate the direct mode, which is of principal interest here. In addition, a few examples will be given of the latest theoretical fits obtained in a direct-reaction computation by Glendenning and Bloom.[14] These will be cited at the end of this section where their significance with regard to the two-body force in the nuclear medium will also be noted.

We should like to begin by examining the strictly qualitative behavior of both the $C^{13}(p,n)N^{13}$ and the $N^{15}(p,n)O^{15}$ angular distributions side by side. This is best done by referring to Fig. 10, where we have combined the data from this experiment with the data on C^{13} from Albert, Bloom, and Glendenning,[8] and also the data on N^{15} from Jones et al.[2] The plots have been made in the same semilog fashion as the previous figures, the energy characterizing each curve being higher with higher vertical position. In this figure, however, the vertical placement of the curve has no quantitative significance, since we wish only to consider the qualitative behavior of the shapes as a function of increasing energy. Also, we wish to compare the angular distributions for C^{13} and N^{15} at equivalent energies and see if this

comparison bears out the twin-reaction hypothesis of Bloom, Glendenning, and Moszkowski.[1] What is meant by "equivalent" energies is best understood by describing briefly the concept of "twin reactions." In the particular direct-reaction mode under investigation here it is the nucleon-nucleon interaction between the incoming proton and the bound neutron (or the bound proton and the outgoing neutron in the final state) which gives rise to the predominant part of the cross section for the process being observed. Thus in the case of C^{13}, if the shell structure of this nucleus is well approximated by a closed sub-shell core of C^{12} with a $P_{1/2}$ neutron external to this core,[15] this interaction is between a free nucleon (either incoming or outgoing) and a bound $P_{1/2}$ nucleon. Similarly, it is not hard to show[1] that for N^{15} the nucleon-nucleon interaction is between a free nucleon and a bound $P_{1/2}$ nucleon <u>hole</u>. It is therefore comparatively easy to see that aside from nuclear size differences and the difference in Q-values in the two cases the direct-reaction cross sections ought to be identical, thus leading to very much the same ("twin") angular distributions and excitation characteristics. In Fig. 10 an attempt has been made to reduce the effect of the difference in Q by adding $Q/2$ to the initial energy in the center-of-mass system, since the total energies of scattering systems before and after collision differ precisely by Q. It must be emphasized that this method of calculating equivalent energies is to be regarded as a necessarily crude approach. We hope that the method will be improved in the near future,[14] particularly since it totally ignores the size factor, which must be at least as important as the Q difference.

Qualitatively both the $C^{13}(p,n)$ and $N^{15}(p,n)$ angular distributions exhibit the expected properties of a direct reaction in that the changes are quite gradual as the bombarding energy is increased. Furthermore, the trend in the angular-distribution complexity is generally to increase with increasing

energy, a characteristic to be expected because higher orbital angular momenta make their contributions to the total cross section more evident with increased momentum available. Since it is not possible to conceive of any first-order direct process outside the residual nucleon-nucleon interaction which could give rise to the (p, n) reaction joining two essentially identical ground states[1] (i. e., C^{13} and N^{13} are charge-mirror images of each other, as are N^{15} and O^{15}), it is already clear that the two-body nucleon-nucleon force must be basically responsible for what has been observed. Further confirmation of this is amply provided by the striking similarity of the C^{13}(p, n) and N^{15}(p, n) angular distributions at the equivalent energies defined above. At the two highest energies shown, the curves for C^{13} and N^{15} seem at first sight almost indistinguishable, in spite of the somewhat complicated shapes which the angular distributions assume here. The close likeness of the two cases continues with the disappearance, almost simultaneously, at the equivalent energy of 8. 2 Mev, of the two peaks in the vicinity of cos $\theta = \pm 0.6$. Between 8. 2 and 6. 4 Mev the similarities are not so clear, but the transition from 5. 9 Mev to 6. 4 Mev for both C^{13} and N^{15} again exhibits almost the identical behavior. Again between 3. 4 and 3. 8 Mev the likeness is quite marked. Unfortunately, for C^{13} data are lacking between 3. 8 and 4. 4 Mev, and since, especially at the lower energies, the rendering of an equivalent energy scale by the method adopted above is more dubious than ever, it would be much more illuminating to have the experimental data and find out empirically the correct energies at which to make these comparisons. Nonetheless the indication seems to be that even at lower energies the N^{15} angular distributions which find their equivalent in the case of C^{13} have much the same equivalent energy (on the scale adopted here) as their C^{13} counterpart. Witness, for example, the 2. 6-Mev curve in C^{13} as compared to the 2. 8-Mev curve in N^{15}. At lower

energies yet, data are again lacking because the N^{15} angular distributions within 200 kev or so of threshold are unknown at this time. These might be interesting in that the pronounced forward peaking observed in this region in the case of C^{13} might indicate,[19] in the twin-reaction picture, a similar phenomenon for N^{15}.

Turning now to the excitation data, which is shown in Fig. 7, we see that in keeping with the above discussion the curves for C^{13} and N^{15} are very similar in both shape and magnitude. Particularly notable is the resonance structure evident in the C^{13} curve at 8.6 Mev and in the N^{15} curve at 7.7 Mev. The N^{15} resonance is less pronounced and appears to be narrower than the C^{13} resonance. However, both resonances have a width of the order of 1 Mev, and making even the most liberal allowances for the cyclotron energy spread would lead to prohibitively large cross sections, should we desire to attribute either or both of these resonances to a single or even a few compound nuclear levels of widths characteristic of this region of excitation. Therefore it seems quite clear that these levels have the character of single-particle or "size" resonances, consonant with the direct-reaction picture described above. Although we can only make crude arguments at best about the relative positions of what we would like to call corresponding single-particle resonances, it is noteworthy that the arguments do at least show that the resonance displacements are in the right direction in going from A = 13 to A = 15. This follows from assuming that the product $(V + e)^{1/2} A^{1/3}$ (which is proportional to KR) will be roughly a constant for any particular resonance in C^{13} and N^{15}, where V is the effective well depth experienced by the free nucleon, e is the kinetic energy of the bombarding particle at infinity, and K is the wave number in the nuclear medium. Though the value of V deduced from the application of this very approximate argument to the actual peak displacement (see Fig. 7) will

be quite low, it must be remembered that in the surface reaction (which the (p, n) process very likely is) the free particle has a small probability of being exposed to the deeper parts of the optical potential, which makes a lowered value of V at least partly understandable. Indeed, theoretical fits to inelastic processes of the type (n, n'), (p, p'),[16, 17] or (p, n),[8] have given abundant indication of a very substantially lowered value being required for V in all instances. An explanation for this effect has been given by Rodberg,[18] who shows that a lowered value for the real part of the optical well is to be expected in inelastic processes as a consequence not only of the surface localization of the reaction, but also of what he calls the 1/A-effect; this effect is the change in the effective optical parameters due to subtracting from the sum total of all interactions between the incoming nucleon and the nucleus that particular nucleon-nucleon interaction which is responsible for the direct process being observed.

In Figs. 8 and 9 the energy variations in the differential cross sections at 40° and 5° have been given. The similarity of the two cases, even to the "fine" structure at 5° between 6 and 8 Mev, is very evident. Otherwise, the general shapes and magnitudes of both curves are the same, but with shifts in energetic positions which almost certainly are not easily explicable without a thorough-going theoretical investigation.

A comparison between theory[14] and experiment is shown in Fig. 11 for the center-of-mass energy of 11.33 Mev for C^{13} and 11.44 Mev for N^{15}. The equivalent energies (defined above) are about the same in the two cases, being 9.8 Mev for the former and 9.7 Mev for the latter, which is the reason why these particular cases were selected for comparison. The parameters of the theoretical calculation[19] are as follows:

Initial State (free proton, bound neutron):

$$V = 40 \text{ Mev, for } C^{13} \text{ and } N^{15};$$
$$W = 6 \text{ Mev, for } C^{13} \text{ and } N^{15}.$$

Final State (free neutron, bound proton):

$$V = 45 \text{ Mev, for } C^{13} \text{ and } N^{15};$$
$$W = 8 \text{ Mev, for } C^{13} \text{ and } N^{15}.$$

V and W are the real and imaginary parts, respectively, of the square well used to generate the distorted wave functions which go into the Born Approximation calculation.[16] The square wells extend out to $R_p = 1.30\, A^{1/3} \times 10^{-13}$ cm, beyond which V and W for both initial and final states become zero. Since the theoretical approach[16,19] assumes a surface interaction, another input parameter of the calculation is the radius of this interaction surface (R_I), which was about 8% larger than R_p for the theoretical curves shown. Finally, the form taken for the residual nucleon-nucleon interaction, which, in the view adopted here, is responsible for the process being observed, is as follows:

$$V_{np} = (V_{so} \Pi_s - V_{to} \Pi_t)\, e^{-\beta r_{np}^2},$$

where Π_s and Π_t are the singlet and triplet projection operators, V_{so} and V_{to} are the amplitudes of each of these components, and β is the range parameter of the gaussian form for the two-particle interaction, assumed to be the same here for both singlet and triplet states. For the theoretical curves shown in Fig. 11, V_{so} was taken to be -30 Mev, V_{to} to be -12 Mev, and β was 0.8 in units of $(\text{fermis})^{-2}$. It is important to emphasize that the above values for V, W, and R_I were obtained by first extrapolating from the fits obtained at lower energies,[8] and then checked with a "goodness-of-fit" calculation using a χ^2-type analysis[14] by varying these parameters around the

extrapolated values. It is interesting and gratifying that not only was the extrapolation vindicated but that the same values for V, W, and R_I turned out to give the best fits for both C^{13} and N^{15}. It is worth noting that the values for V and W are surprisingly close to the elastic-scattering parameters (see e.g., Glassgold[20]), although the precise significance of this is obscured by the fact that the (p,n) process and elastic scattering have basic differences. Nonetheless at lower energies it was found[8] that V was very significantly reduced as compared to the elastic-scattering parameters — in keeping with the results of Levinson and Banerjee[17] and Glendenning.[16]

With regard to the determination of V_{np}, it is essential to remember that absolute cross sections could not be predicted with any reliability using a square-well wave-generating routine because of the sharp and artificial reduction of the wave amplitudes for radii greater than R_p. Fortunately this does not seriously impair the validity of the theoretical predictions of relative angular distributions, nor does it affect seriously the ratio V_t/V_s, which was determined to give the best fit (by the same χ^2-type analysis mentioned above) at the value of about +0.40. This value was found to give the best fit also at four lower energies, ranging from 4.1 to 8.6 Mev. Furthermore, this ratio was very largely independent of changes in V, W, R_p, or R_I. Because of this insensitivity, it is felt that the (p,n) reactions on mirror nuclei do indeed offer an excellent prospect of usefully investigating the two-body force in the nuclear medium, as originally proposed.[1] The relation between (V_t/V_s) as determined here and as determined from free-scattering experiments[8, 21] (about +0.6) is far from obvious, but it does not seem too much to expect[18] that in the near future techniques will be worked out to elucidate this relationship. The closeness of the two V_t/V_s ratios would seem to suggest that the nuclear medium does

not materially alter the "free" neutron-proton force. However, the role of the neglected tensor force[8] remains to be determined.

Note: After completion of this manuscript, it was discovered that Dagley et al. (Proceedings of the International Conference on Nuclear Structure, Kingston, Canada, August 29–September 3, 1960) have done a rather complete job on the $C^{13}(p,n)N^{13}$ ground-state reaction. Their results (obtained with much thinner targets) are in excellent agreement with the results presented in this paper.

FOOTNOTES

* This work was performed under the auspices of the U. S. Atomic Energy Commission.

† A preliminary account of this work was presented at the American Physical Society 1960 Montreal meeting: Bull. Am. Phys. Soc. 5, 346 (1960).

[1] S. D. Bloom, N. K. Glendenning, and S. A. Moszkowski, Phys. Rev. Letters 3, 98 (1959).

[2] K. W. Jones, L. J. Lidofsky, and J. L. Weil, Phys. Rev. 112, 1252 (1958).

[3] J. H. Gibbons and R. L. Macklin, Phys. Rev. 114, 571 (1959).

[4] Blaser, Boehm, Marmier, and Scherrer, Helv. Phys. Acta 24, 465 (1951).

[5] S. D. Bloom, R. M. Lemmon, and S. A. Moszkowski, Bull. Am. Phys. Soc. 3, 418 (1958).

[6] J. K. Bair, J. D. Kington, and H. B. Willard, Phys. Rev. 90, 575 (1953).

[7] Dagley, Haeberli, Saladin, and Borchers, Bull. Am. Phys. Soc. 5, 245 (1960).

[8] S. D. Bloom and R. D. Albert, Bull. Am. Phys. Soc. 4, 321 (1959); R. D. Albert, S. D. Bloom, and N. K. Glendenning (to be published).

[9] J. K. Bair, H. O. Cohn, and H. B. Willard, Phys. Rev. 119, 2026 (1960).

[10] F. Ajzenberg-Selove and T. Lauritsen, Nuclear Phys. II, 1 (1959).

[11] Wong, Anderson, Gardner, McClure, and Nakada, Phys. Rev. 116, 164 (1959).

[12] Elwyn, Kane, Ofer, and Wilkinson, Phys. Rev. 116, 1490 (1959).

[13] We are indebted to Robert Kaifer of this laboratory for developing the proton-electron discrimination circuit.

[14] N. K. Glendenning and S. D. Bloom (private communication).

[15] M. K. Banerjee and C. A. Levinson, Ann. Phys. 2, 499 (1957).

[16] N. K. Glendenning, Phys. Rev. 114, 1297 (1959).

[17] C. A. Levinson and M. K. Banerjee, Ann. Phys. 3, 67 (1960).

[18] Leonard S. Rodberg, Ann. Phys. 9, 373 (1960).

[19] An introductory discussion of the calculation is given in Footnote 1. A fuller discussion is given by Albert, Bloom, and Glendenning (Phys. Rev., to be published), wherein the meaning of all the parameters used in this paper is discussed in detail.

[20] A. E. Glassgold, Prog. in Nuclear Phys. 7, 123 (1959).

[21] J. L. Gammel and R. L. Thaler, Prog. in Cosmic Ray Phys. 5, 99 (1960).

/md

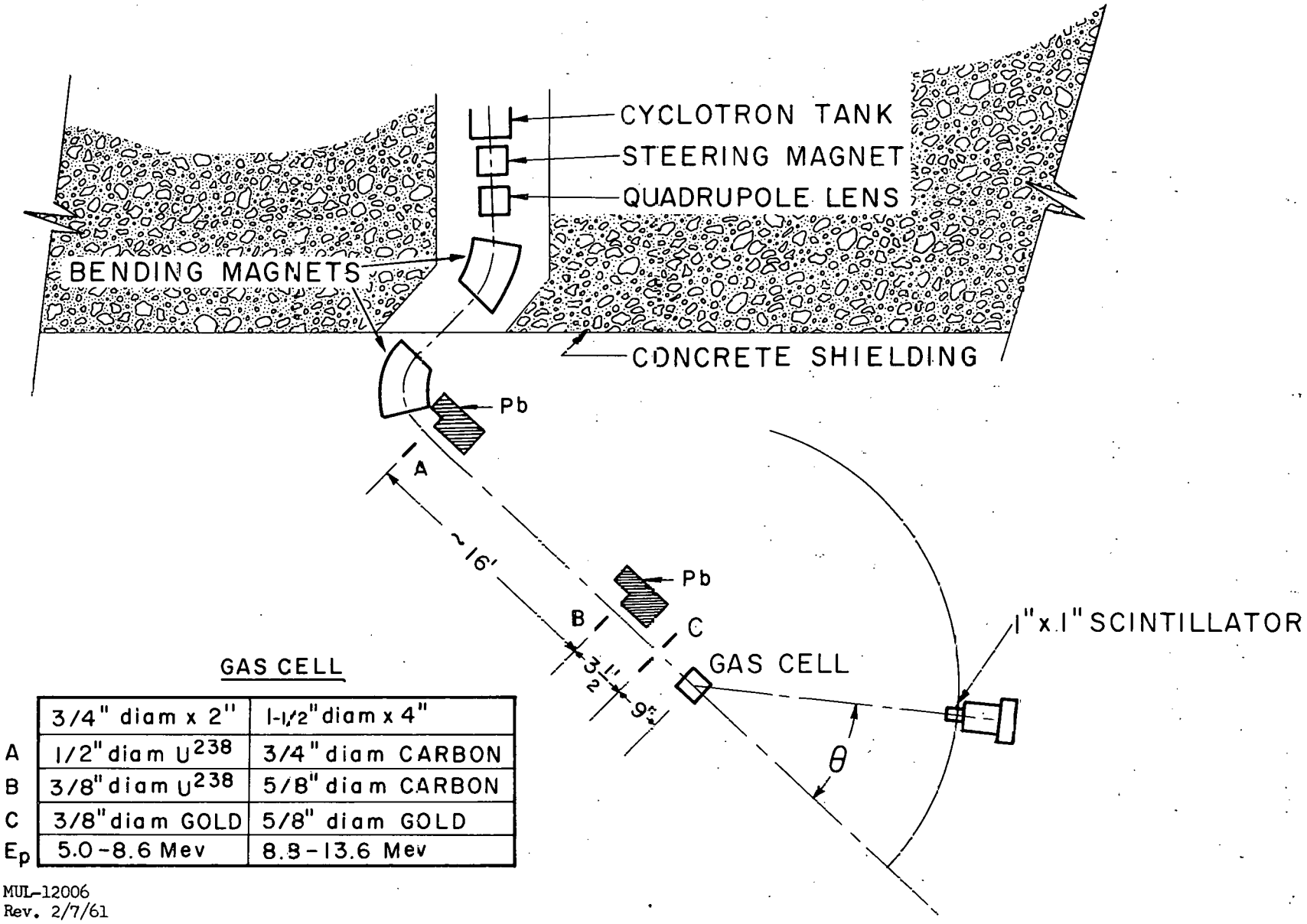

GAS CELL

	3/4" diam x 2"	1-1/2" diam x 4"
A	1/2" diam U^{238}	3/4" diam CARBON
B	3/8" diam U^{238}	5/8" diam CARBON
C	3/8" diam GOLD	5/8" diam GOLD
E_p	5.0 - 8.6 Mev	8.8 - 13.6 Mev

MUL-12006
Rev. 2/7/61

Fig. 1. Schematic diagram of the experimental geometry. The gas cell dimensions, collimator materials, and collimator sizes are indicated in the above table.

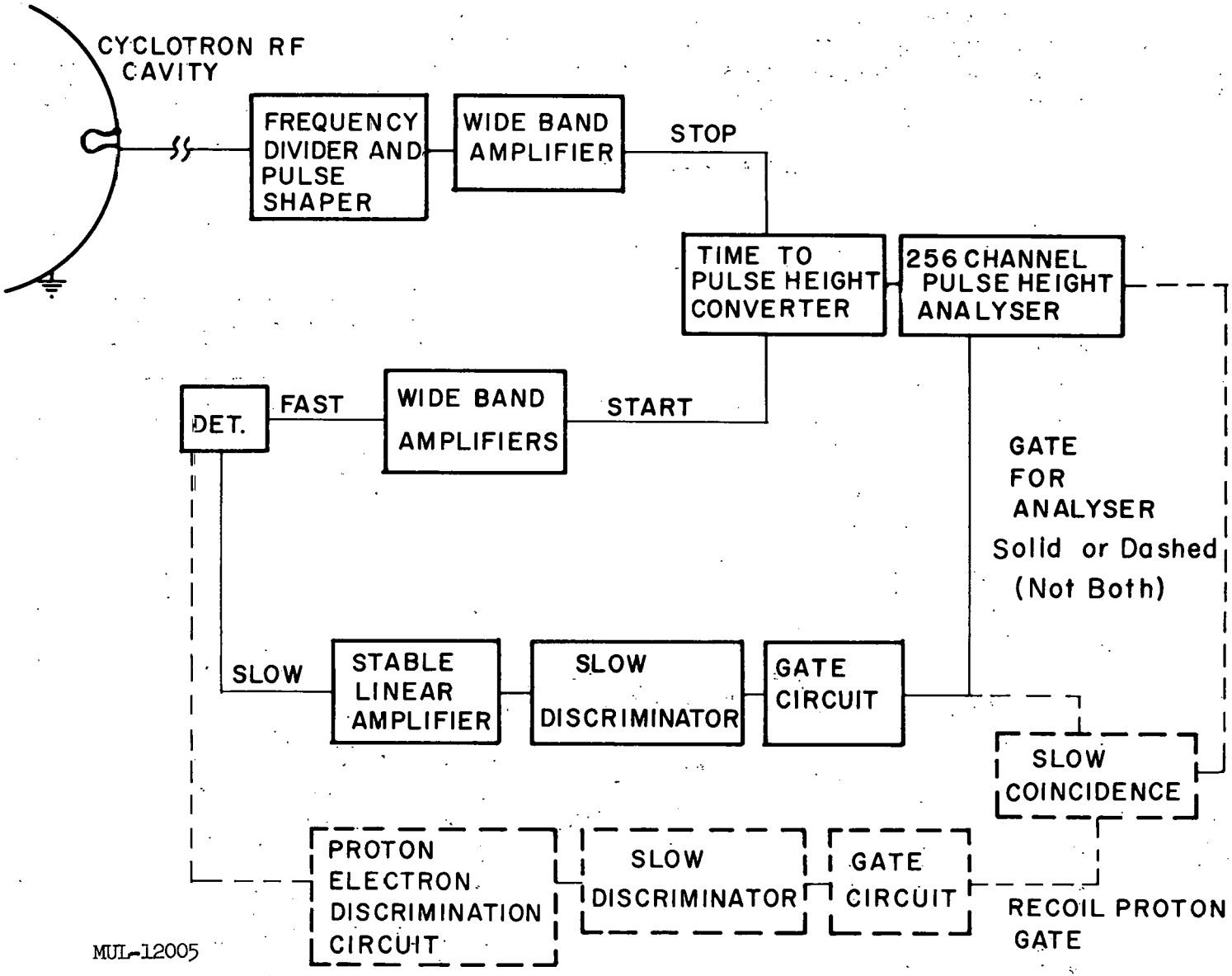

Fig. 2. Schematic diagram of the time-of-flight electronics. The dashed portion was added at the higher proton bombarding energies in order to suppress the copious gamma-ray background.

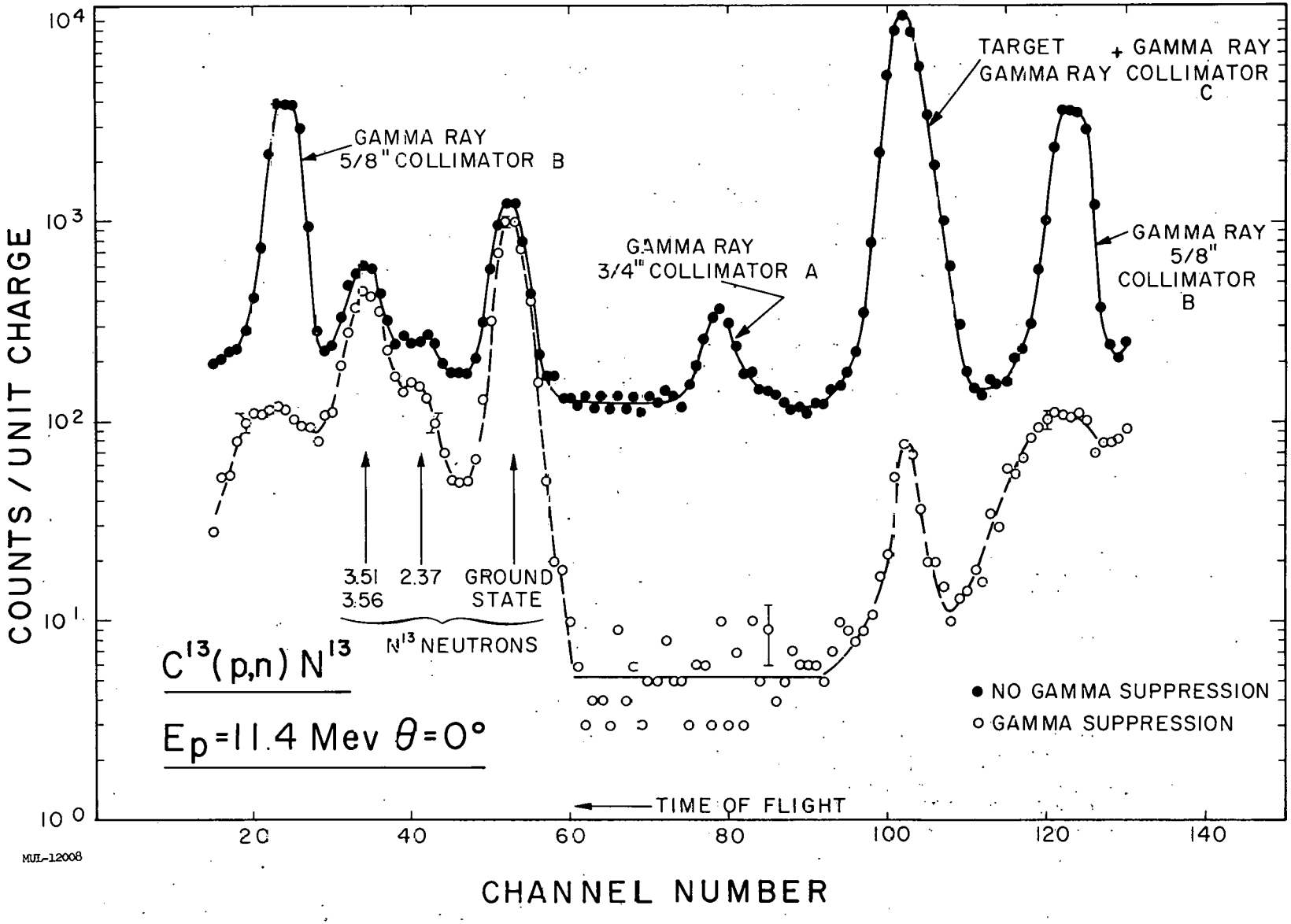

Fig. 3. Time-of-flight spectrum for C^{13} - p at zero degrees and 11.4-Mev protons. Upper and lower curves were taken without and with gamma suppression, respectively. Time calibration of the system is 1.13 millimicroseconds/channel, and increasing time of flight is toward the left. The flight path was 2.5 meters, and the neutron detector bias was 3.15 Mev.

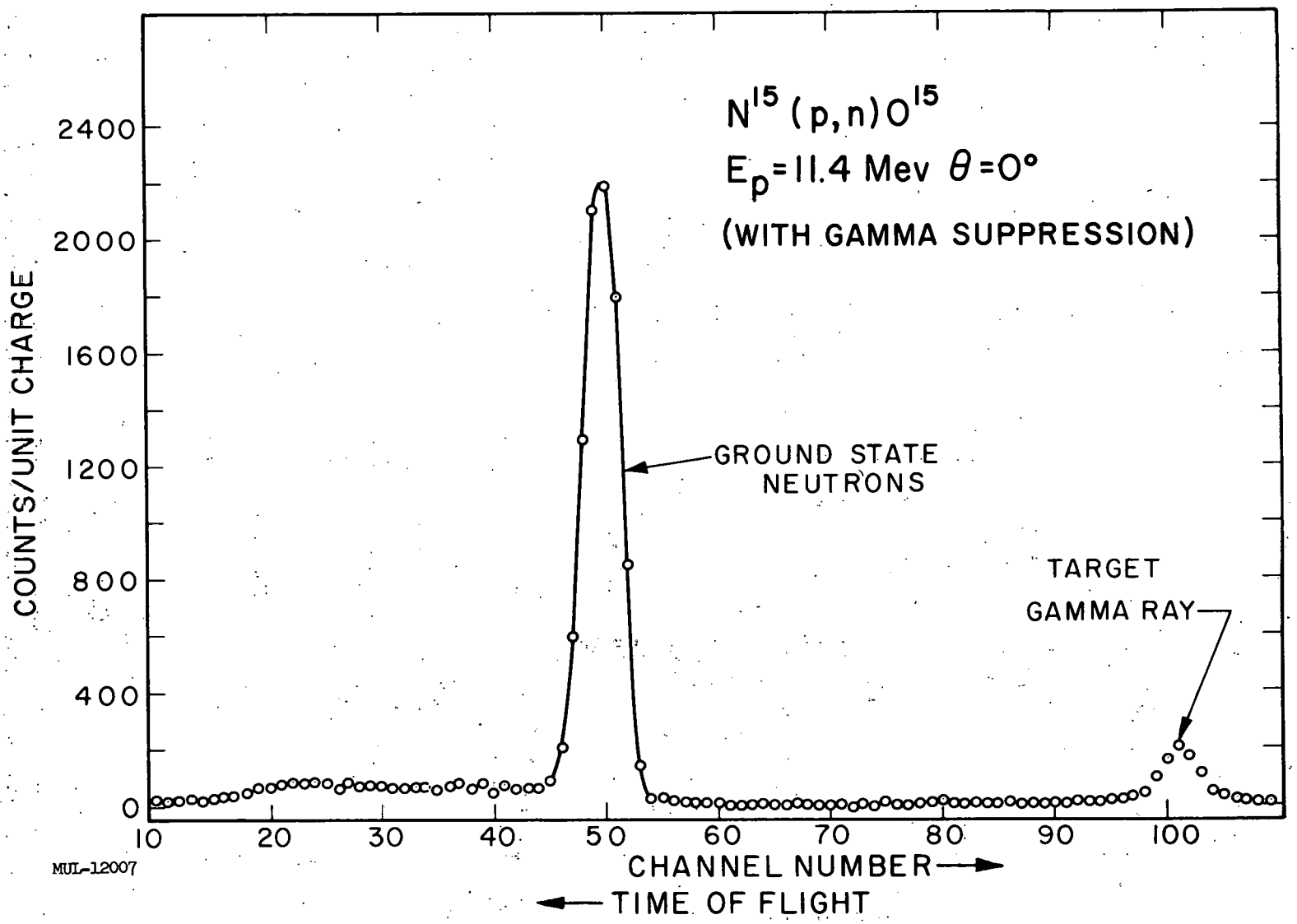

Fig. 4. Time-of-flight spectrum for N^{15} + p at zero degrees and 11.4-Mev protons, employing gamma suppression. See Fig. 3 for time calibration, flight path, and detector bias.

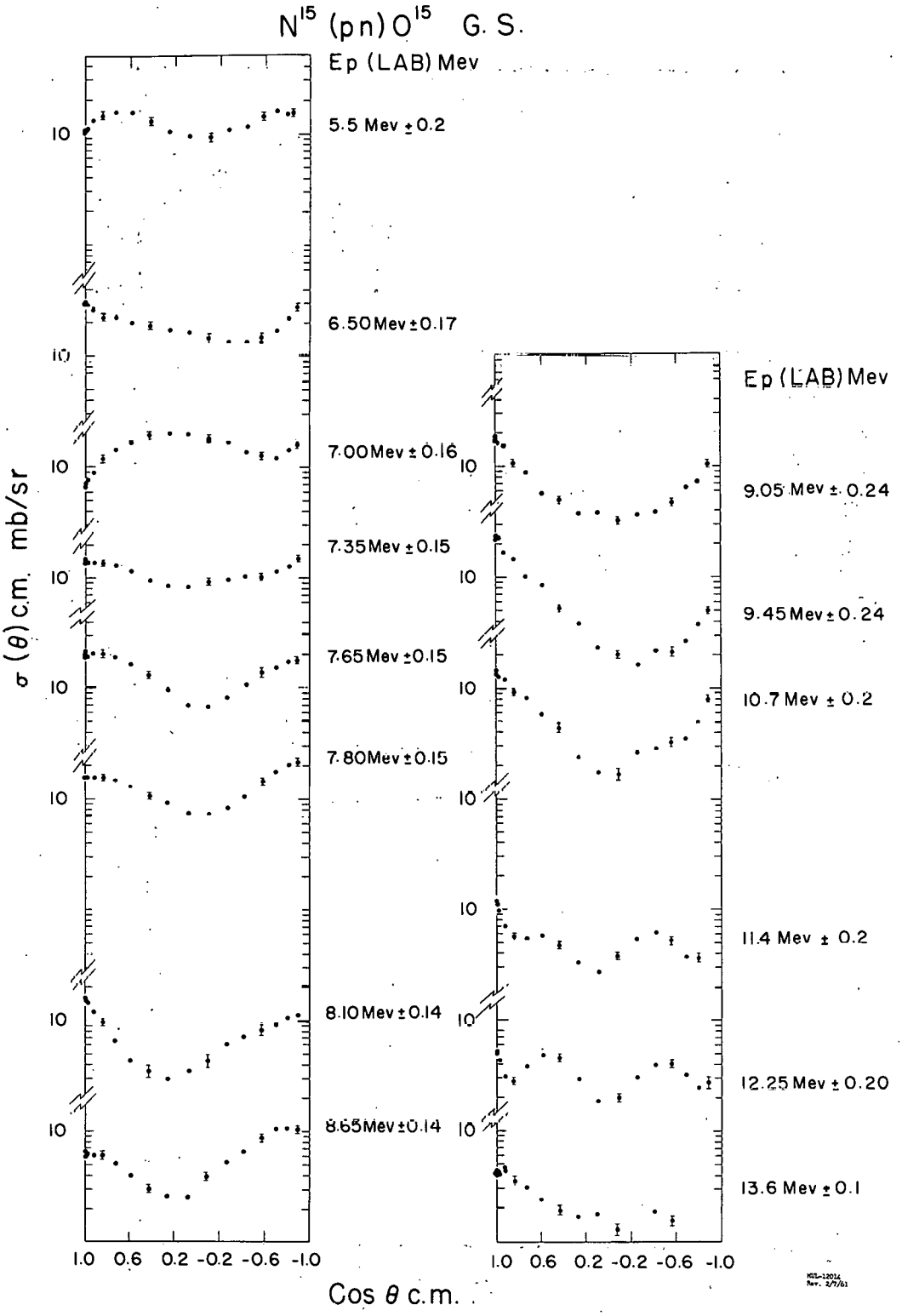

Fig. 5. Center-of-mass absolute differential cross sections for $N^{15}(p,n)O^{15}$ ground-state neutrons versus laboratory bombarding energy. The indicated beam energy spreads are due to energy loss in the gas targets.

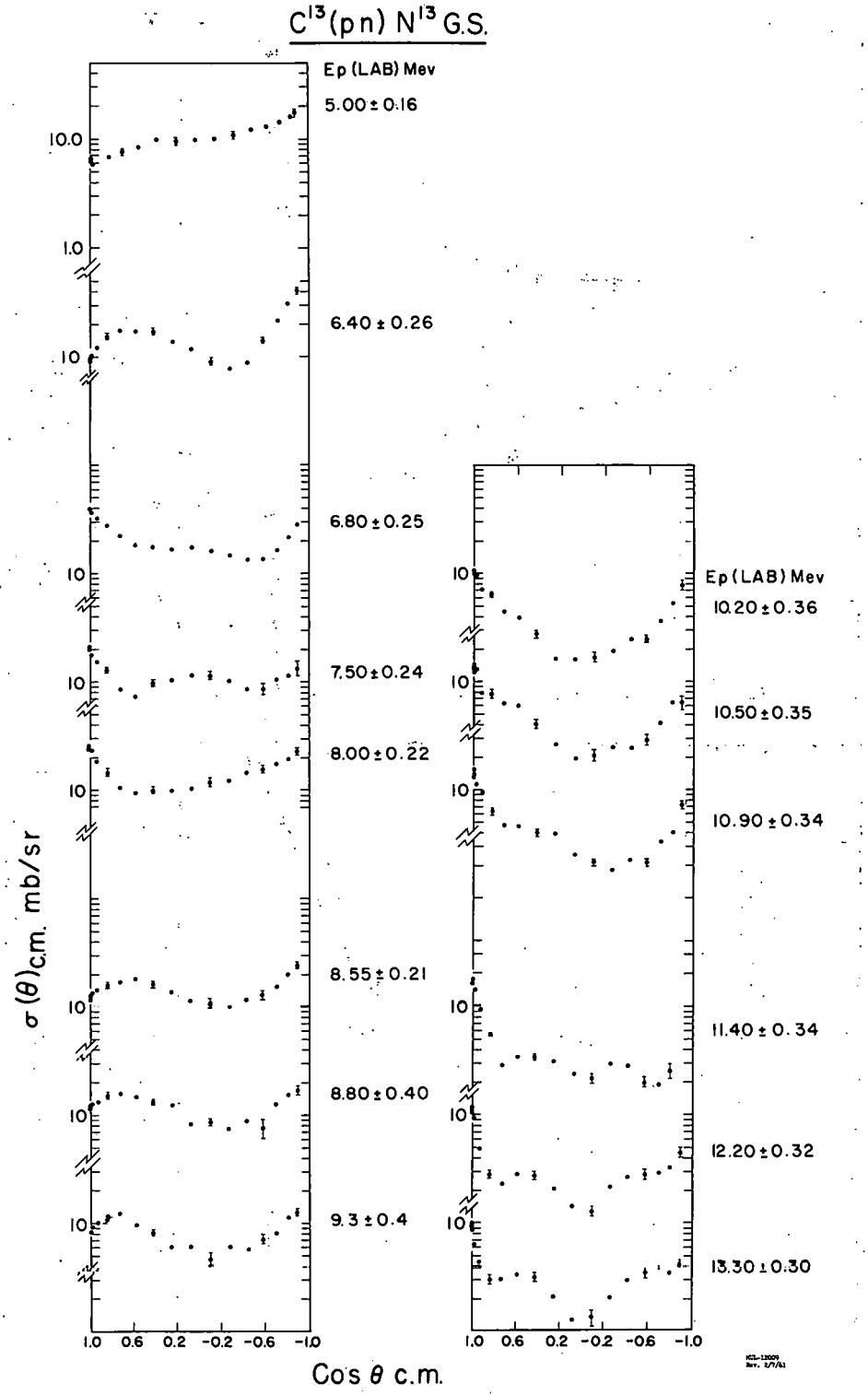

Fig. 6. Center-of-mass absolute differential cross sections for $C^{13}(p,n)N^{13}$ ground-state neutrons versus laboratory bombarding energy. The indicated beam energy spreads are due to energy loss in the gas targets.

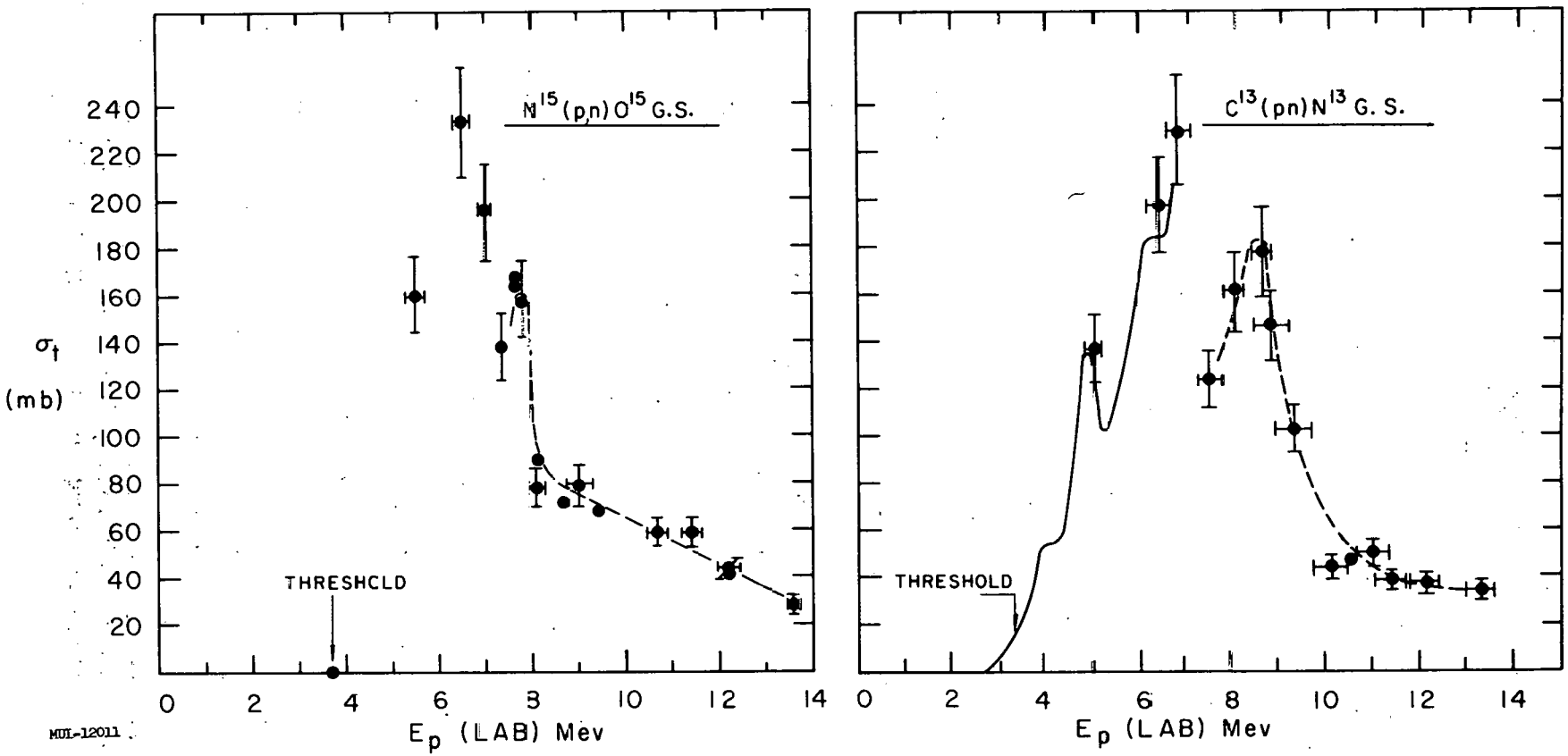

Fig. 7. Total ground-state yield of neutrons from the $C^{13}(p,n)N^{13}$ and $N^{15}(p,n)O^{15}$ reactions. The horizontal bars indicate the energy spreads of the various measurements.

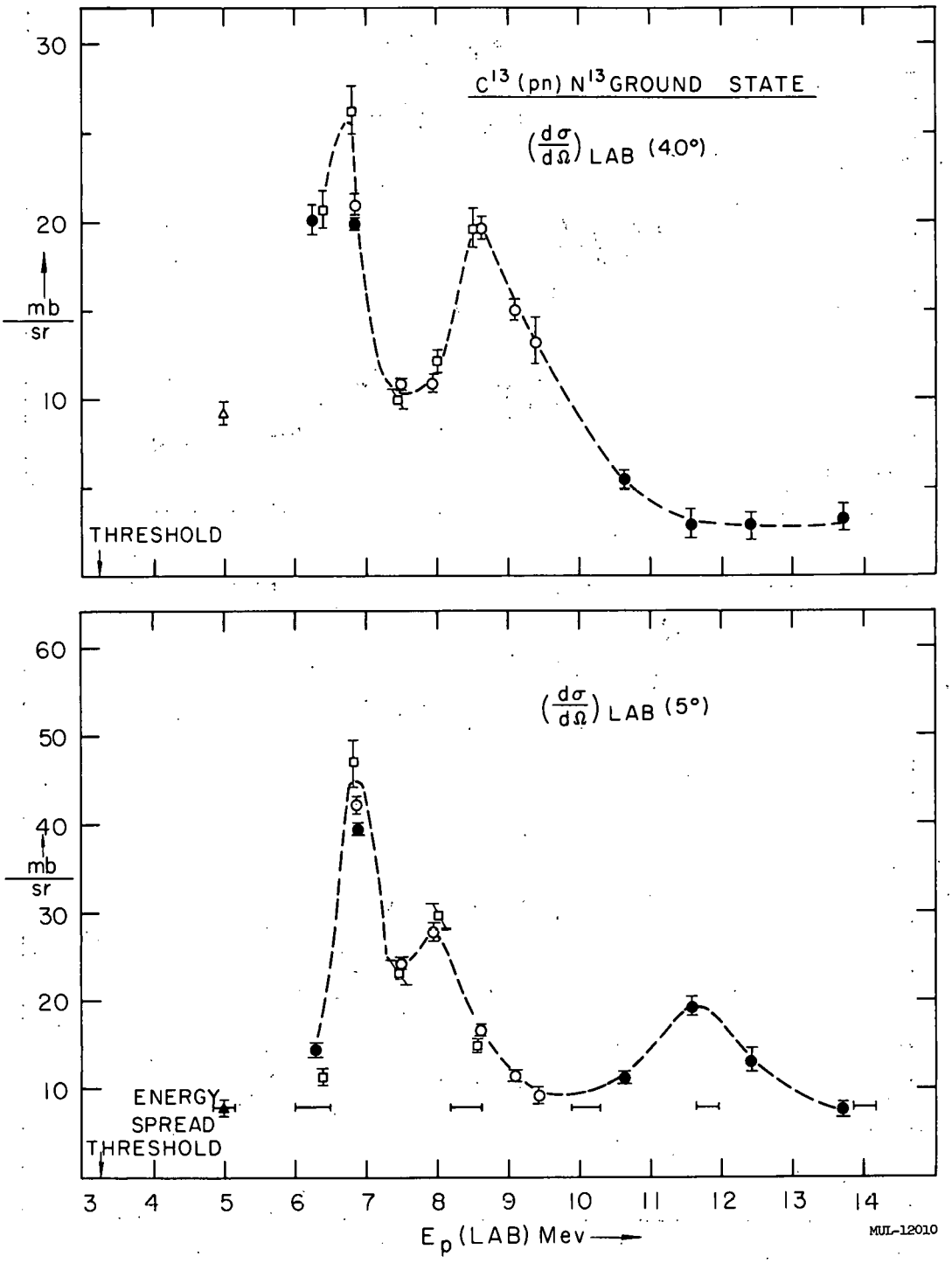

Fig. 8. Differential excitation functions for $C^{13}(p,n)N^{13}$ ground-state neutrons at 5° and 40°. The energy spreads are indicated by the horizontal bars. The 5.0-Mev measurement was made with the gas target filled to one-half an atmosphere of CO_2. See text for the significance of the dashed curves.

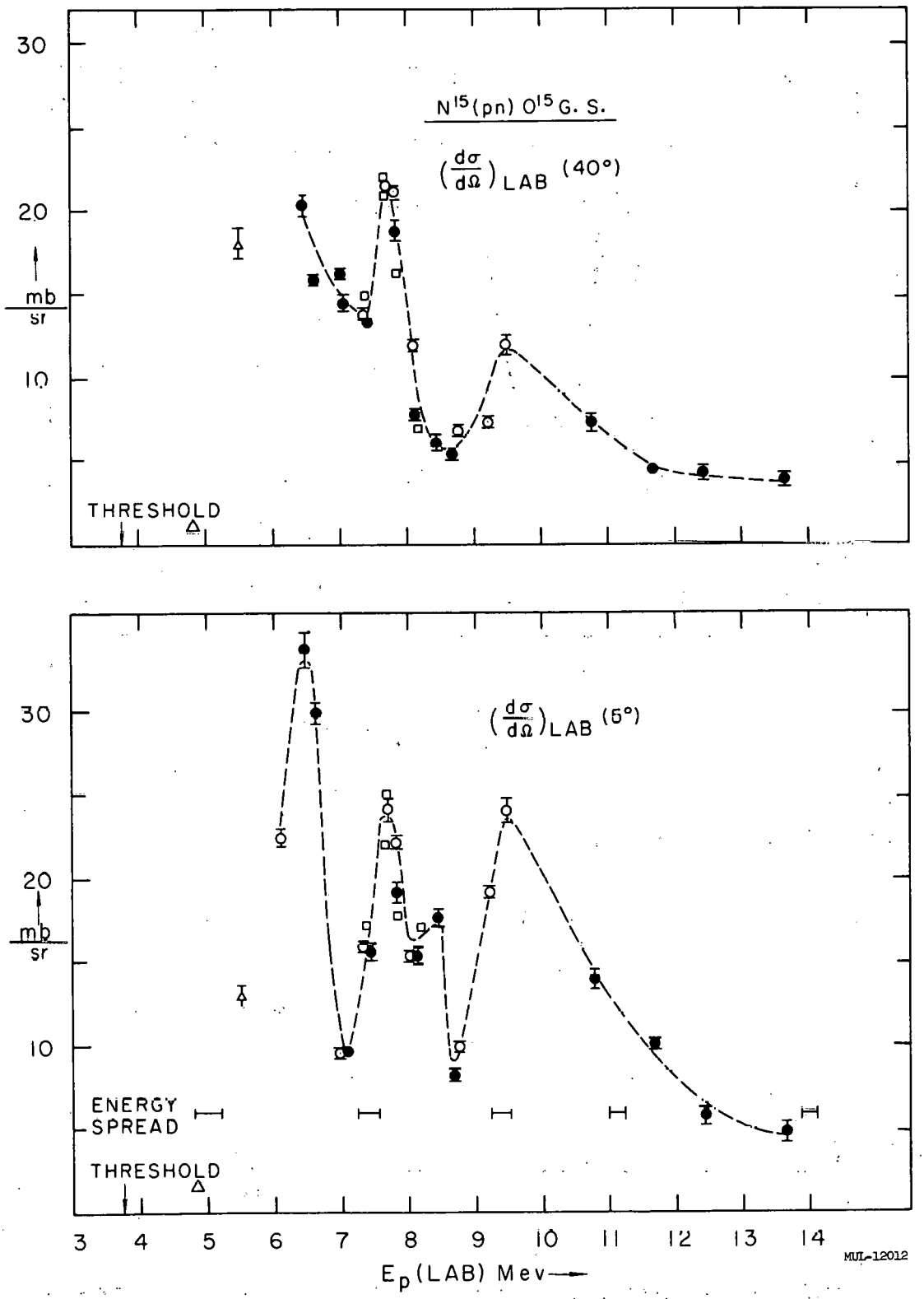

Fig. 9. Differential excitation functions for $N^{15}(p,n)O^{15}$ ground-state neutrons at 5° and 40°. The energy spreads are indicated by the horizontal bars. See text for the significance of the dashed curves.

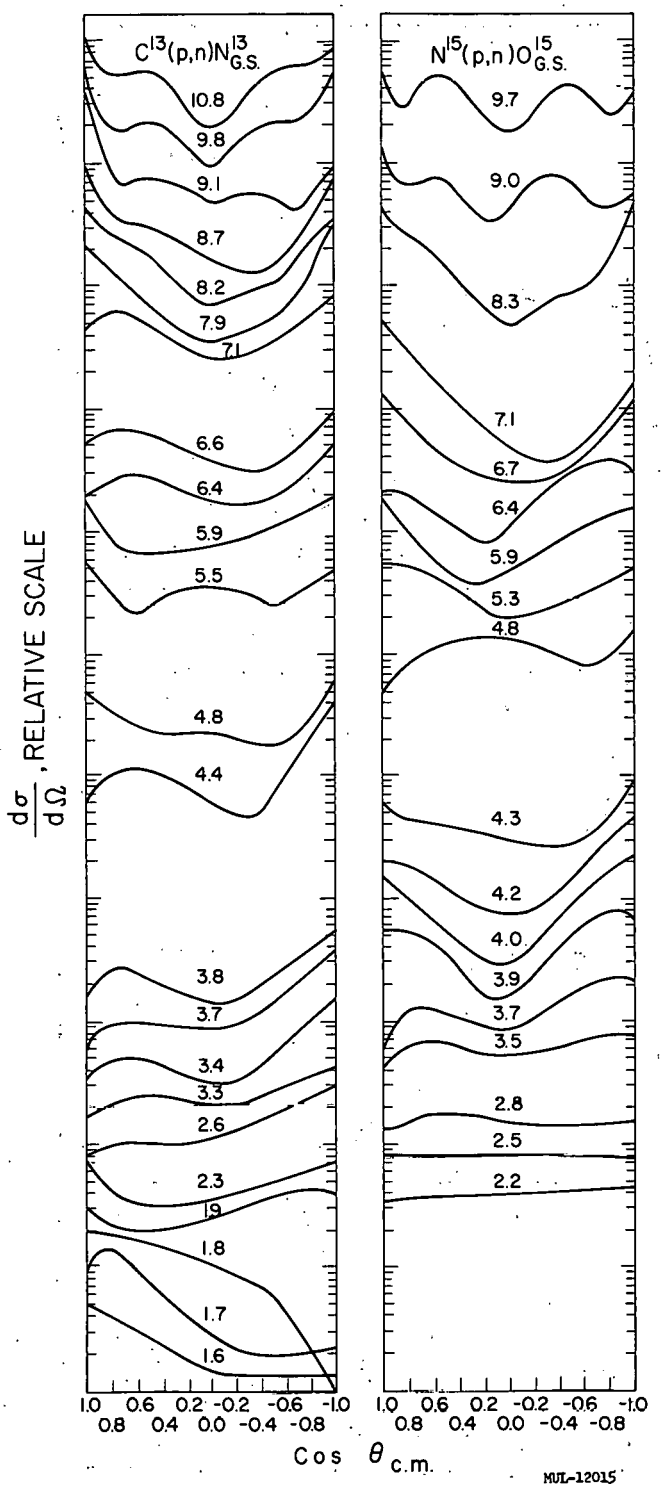

Fig. 10. Comparison of the $C^{13}(p,n)$ and $N^{15}(p,n)$ ground-state angular distributions. The curves are labeled with the "equivalent energy" in order to facilitate the comparison. For N^{15}, the data below an equivalent energy of 4.3 Mev are due to Jones et al.[2] Similarly, the data below 4.4 Mev for C^{13} are due to Albert et al.[8]

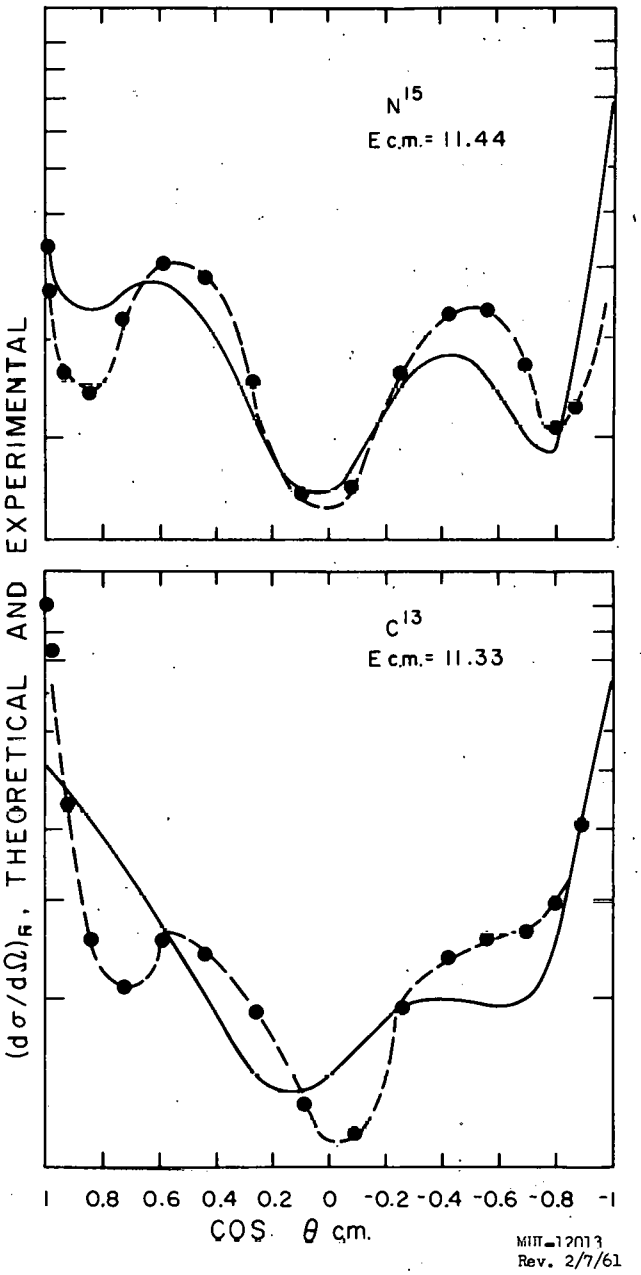

Fig. 11. Comparison of theoretical and experimental angular distributions at the center-of-mass energy of 11.33 Mev for C^{13} and 11.44 Mev for N^{15}. The plots are made on a vertical log scale so as to preserve shape independently of vertical position. The theoretical curves have been moved vertically so that the total theoretical and experimental cross sections are equal in each case. The only significance of the ordinate scale is that it correctly gives the ratios of the cross sections at different angles. Experimental points are joined by a dashed curve for visual ease and the solid curves are theoretical predictions. Accuracy of all experimental points is 10% or better.